Peristaltic transport of a Casson fluid in an asymmetric channel*

P. Naga Rani and G. Sarojamma

Department of Applied Mathematics, Sri Padmavati Women's University, Tirupati, India

Abstract

The peristaltic transport of a Casson fluid in a two - dimensional asymmetric channel is studied under long- wavelength and low-Reynolds number assumption. The asymmetry in the channel is created by considering the peristaltic waves imposed on the boundary walls to possess different amplitude and phase. The analysis of the flow is carried out in a wave frame of reference moving with the velocity of the wave. Due to the asymmetry in the channel two yield planes exist and they are calculated by solving the transcendental equation in terms of the core width. In an asymmetric channel the yield planes are skewed towards the boundary with higher amplitude or a phase difference in relation to the other boundary. While in a symmetric channel the yield planes are located symmetrically on either side of the axis of the channel. The phenomena of trapping and reflux have been discussed in the symmetric case of the channel. It is noticed that trapping of fluid occurs and the trapping zone extends for an increase in the time average flux. It is found that reflux occurs for higher values of amplitude of the peristaltic wave and the reflux zone extends for increased amplitudes.

Key words casson fluid, peristalsis, asymmetric channel, mathematical modelling

Introduction

The phenomenon of peristalsis is well known to physiologists and engineers as one of the major mechanism for transport of fluid in several biological systems and industrial pumping. The peristaltic pumping of a fluid in a distensible tube occurs by a progressive wave of contraction and expansion along the tube. Peristalsis is an inherent property of many biological systems consisting of smooth tubes, which transports bio-fluids by its propulsive movements. The peristaltic mechanism can be found in the transport of urine from kidney to bladder through the ureter, the movement of chyme in the gastrointestinal tract, transport of lymph in the lymphatic vessels, the intra-uterine fluid motion, vasomotion of the small blood vessels and in several other glandular ducts. In industry the peristaltic mechanism is applied to transport corrosive fluids where the contact of fluid with the machinery parts is prohibited, slurries, noxious fluids in the nuclear industry and sanitary fluids. Based on the principle of peristalsis mechanical roller pumps, heart–lung machines, cell separators etc. have been fabricated.

Following the first study of Latham[9] on peristalsis, several experimental and theoretical studies were developed to understand the fluid mechanical aspects of peristaltic transport in different situations. Many of these studies deal with the characteristics of pumping, reflux and trapping. Most of these studies have been carried out by treating that blood and other physiological fluids as Newtonian fluids. Although this approach provides a satisfactory understanding of the peristaltic mechanism in the ureter, it fails to provide a satisfactory model to describe the peristaltic mechanism in small blood vessels, lymphatic vessels and other glandular ducts. The study of peristalsis through non-Newtonian fluids is significant as blood in small arteries and fluids in the lymphatic vessels, intestine, urine under certain pathological conditions etc. behave as non-Newtonian fluids. Modelling of these fluids as non-Newtonian provides a realistic model. Raju and Devanathan[15] are the first researchers to study the peristaltic transport of non-Newtonian fluids. Srivastava[17] investigated the problem of peristaltic transport of blood by assuming a single layer/ Canada Casson fluid, which ignores the presence of peripheral layer. Srivastava and Srivastava[18] studied the peristaltic transport of blood in a uniform and non-uniform tube, when blood is represented by a two-layered fluid model, consisting of a core region of suspension of all erythrocytes, assumed to be a Casson fluid, and peripheral layer of plasma as a Newtonian fluid.

*Presented at the XI congress of Andhra Pradesh Society for Mathematical Sciences, Tirupati, A.P. India, 31 Jan-2 Feb 2003
Corresponding author: G. Sarojamma, Department of Applied Mathematics, Sri Padmavati Mahila Women's University, Tirupati-517 502, A. P., India,
Email: nagarani_ponakala@yahoo.co.in
Received: 8 June 2003; Accepted: 28 June 2004

Siddique *et al.*[19] analysed the peristaltic motion of a non-Newtonian fluid modelled with a constitutive equation for a second order fluid in a planar channel. Tang and Rankin[20] proposed mathematical model for peristaltic transport of a nonlinear viscous flow where they used iterative methods to solve a free boundary problem. Elshehawey *et al.*[5] analysed the peristaltic transport of a non-Newtonian (Carreau) fluid in a non-uniform channel under zero Reynolds number with long wavelength approximation. Mernone and Mazumdar[10] analysed a mathematical model for the peristaltic transport of a Power law fluid in a planar geometry. In their subsequent papers[11, 12] they studied the peristaltic transport of a Casson fluid in a two-dimensional channel using the generalized form of constitutive equation for Casson fluid, proposed by Fung[7, 8].

The peristaltic transport of fluids in asymmetric channels has application in physiology. In the studies of De Vries *et al.*[4] it was mentioned that the intra-uterine contraction due to myometrial contraction is peristaltic type motion and the myometrial contractions may occur in both symmetric and asymmetric directions. Eytan and Elad[6] studied the wall - induced peristaltic fluid flow in a planar channel with wave trains having a phase difference moving independently on the upper and lower walls to simulate intra-uterine fluid motion in a sagittal cross -section of the uterus. Pozrikidis[14] analysed the peristaltic transport of a viscous fluid in an asymmetric channel under long-wavelength and low-Reynolds number assumptions. The flow was investigated in a wave frame of reference moving with the velocity of the wave and the effects of phase difference, varying channel width and wave amplitudes on the pumping characteristics, streamline pattern, trapping and reflux were discussed. Mishra and Rao[13] studied the peristaltic transport of an incompressible viscous fluid in an asymmetric channel under long-wavelength and low-Reynolds number assumptions. The flow was investigated in a wave frame of reference moving with velocity of the wave and the effects of phase difference, varying channel width and wave amplitudes on the pumping characteristics, streamline pattern, trapping and reflux were discussed.

In this paper the peristaltic transport of a Casson fluid in a two-dimensional asymmetric channel is studied under long-wavelength and low-Reynolds number assumption. The motivation for studying this problem is to understand the effects of peristalsis on the flow characteristics of physiological fluids modelled as a Casson fluid. The results in symmetric and asymmetric channels are discussed. The results are compared and found to be in agreement with those of Shapiro *et al.* [16] when the channel is symmetric and the fluid is Newtonian with Mernone and Mazumdar[12] in the case of a symmetric channel and with those of Mishra and Rao[13] in the Newtonian fluid case.

Mathematical formulation

We consider the peristaltic transport of a non-Newtonian fluid, modelled as a Casson fluid in a two dimensional channel, (shown in Fig.1) induced by sinusoidal wave trains propagating with constant speed c along the channel walls defined by

$$Y = H_1 = d_1 + a_1 \cos\frac{2\pi}{\lambda}(X - ct) \quad (1a)$$

$$Y = H_2 = -d_2 - b_1 \cos\left(\frac{2\pi}{\lambda}(X - ct) + \phi\right) \quad (1b)$$

where a_1, b_1 are the amplitudes of the waves, λ is the wave length $d_1 + d_2$ is the width of the channel, ϕ is the phase difference which varies in the range $0 \le \phi \le \pi$. $a_1 = b_1$, $d_1 = d_2$, $\phi = 0$, correspond to a symmetric channel. Under the assumption of infinite wavelength and neglecting the inertial terms the equations of motion reduce to

$$\rho\frac{\partial U}{\partial t} = -\frac{\partial P}{\partial X} - \frac{\partial}{\partial Y}(Y\tau) \quad (2a)$$

$$\frac{\partial P}{\partial Y} = 0 \quad (2b)$$

where ρ is the density, U is the axial velocity, t is the time, P is the pressure and τ is the shear stress. In order to obtain the flow fields completely the constitutive equation is required.

Casson's constitutive equation

The Casson's constitutive equation corresponding to the flow is given by

$$\tau^{\frac{1}{2}} = \tau_y^{\frac{1}{2}} + \left(-\mu_\infty\frac{\partial U}{\partial Y}\right)^{\frac{1}{2}} \quad \text{if } \tau \ge \tau_y \quad (3a)$$

$$\frac{\partial U}{\partial Y} = 0 \quad \text{if } \tau \le \tau_y \quad (3b)$$

where τ_y is the yield stress and μ_∞ is the Newtonian viscosity (viscosity at high rate of shear). From the relation (3b) it is seen that the velocity gradient vanishes in the region where the shear stress is less than the yield stress. As a result plug flow sets in whenever $\tau \le \tau_y$. The above relations between the shear stress and shear rate $\frac{\partial U}{\partial Y}$ are appropriate for positive values of τ and negative values of $\frac{\partial U}{\partial Y}$. The equivalent form of these relations for more general situation where the shear stress and shear rate can

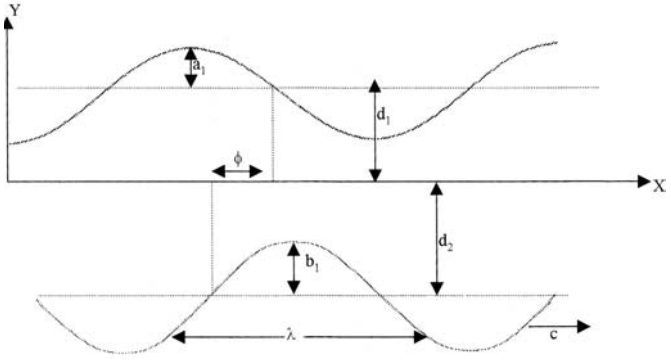

Figure 1. *Schematic diagram of a two dimensional asymmetric channel.*

change the sign (as in the case of a annulus, Bird *et al.*[3]) may be written as (Aroesty and Gross[1, 2])

$$\mu_\infty \frac{\partial U}{\partial Y} = -\left(1 + \frac{\tau_y}{|\tau|} - 2\frac{\tau_y^{1/2}}{|\tau|^{1/2}}\right)\tau \quad \text{if} \quad \tau \geq \tau_y \tag{4a}$$

$$\frac{\partial U}{\partial Y} = 0 \qquad \text{if} \quad \tau \leq \tau_y \tag{4b}$$

It is clear from equation (4) that the flow of a Casson fluid in the asymmetric channel is three phase in nature in which the central core region corresponds to the plug region. If the plug region is represented by $\lambda_1 \leq Y \leq \lambda_2$ where $H_2 \leq \lambda_1, \lambda_2 \leq H_1$, and the two shear flow regions by $H_2 \leq Y \leq \lambda_1$ and $\lambda_2 \leq Y \leq H_1$, then the Casson's constitutive equation (4) in these regions can be rewritten as

$$\mu_\infty \frac{\partial U}{\partial Y} = -\tau + \tau_y - 2\tau_y^{1/2}|\tau|^{1/2} \quad \text{if } H_2 \leq Y \leq \lambda_1 \tag{5a}$$

$$\frac{\partial U}{\partial Y} = 0 \qquad \text{if } \lambda_1 \leq Y \leq \lambda_2 \tag{5b}$$

$$\mu_\infty \frac{\partial U}{\partial Y} = -\left(\tau + \tau_y - 2\tau_y^{1/2}\tau^{1/2}\right) \text{ if } \lambda_2 \leq Y \leq H_1 \tag{5c}$$

$Y = \lambda_1$ and $Y = \lambda_2$ are the two yield plane locations to be determined as part of solution to the problem under investigation.

The corresponding boundary conditions are given by

$$U(Y = H_1) = 0 = U(Y = H_2) \tag{6a}$$

$$-\tau\,(Y = \lambda_1) = \tau_y = \tau\,(Y = \lambda_2) \tag{6b}$$

$$U(Y = \lambda_1) = U(Y = \lambda_2) = U_p \tag{6c}$$

where U_p is the plug flow velocity.

If the tube length is finite but equal to an integral number of wavelengths, and if the pressure difference between the ends of the tube is constant, the flow is steady in the wave frame (Shapiro *et al.*[16]). We assume that these conditions are met, and we study the problem in the wave frame. The transformations between fixed frame O(X, Y) and moving frame o(x, y) are given by

$$x = X - ct, \quad y = Y \tag{7a}$$

$$u(x, y) = U(X - ct, Y) - c, \quad v(x, y) = V(X - ct, Y) \tag{7b}$$

and $p(x) = P(X, t)$, where (u, v) and (U, V) are velocity components, p and P are pressures in wave and fixed frame of references respectively. The pressure p remains a constant across any axial station of the channel under the assumption that the wavelength is large and the curvature effects are negligible.

We introduce the following non-dimensional quantities:

$$\bar{x} = \frac{x}{\lambda}, \quad \bar{y} = \frac{y}{d_1}, \quad \bar{u} = \frac{u}{c}, \quad \bar{v} = \frac{v}{c\delta}, \quad \delta = \frac{d_1}{\lambda}$$

$$\bar{p} = \frac{d_1^2 p}{\mu_\infty c \lambda}, \quad \bar{\tau} = \frac{\tau}{\mu_\infty c/d_1}, \quad \bar{\tau}_y = \frac{\tau_y}{\mu_\infty c/d_1}, \quad h_1 = \frac{H_1}{d_1},$$

$$h_2 = \frac{H_2}{d_1}, \tag{8}$$

$$d = \frac{d_2}{d_1}, \; a = \frac{a_1}{d_1}, \; b = \frac{b_1}{d_1}, \quad \bar{\lambda}_1 = \frac{\lambda_1}{d_1}, \quad \bar{\lambda}_2 = \frac{\lambda_2}{d_1}$$

After dropping bars, the non-dimensional wall equations are given by

$$y = h_1 = 1 + a\cos(2\pi x) \tag{9a}$$

$$y = h_2 = -d - b\cos(2\pi x + \phi) \tag{9b}$$

The equations of motion in dimensionless form, become

$$\frac{\partial p}{\partial y} = 0 \tag{10a}$$

$$-\frac{\partial p}{\partial x} - \frac{\partial \tau}{\partial y} = 0 \tag{10b}$$

The Casson's constitutive equation in the non-dimensional form is

$$\frac{\partial u}{\partial y} = -\tau + \tau_y - 2\tau_y^{1/2}|\tau|^{1/2} \quad \text{if } h_2 \leq y \leq \lambda_1 \tag{11a}$$

$$\frac{\partial u}{\partial y} = 0 \qquad \text{if } \lambda_1 \leq y \leq \lambda_2 \tag{11b}$$

$$\frac{\partial u}{\partial y} = -\left(\tau + \tau_y - 2\tau_y^{1/2}\tau^{1/2}\right) \text{ if } \lambda_2 \leq y \leq h_1 \tag{11c}$$

The corresponding boundary conditions in non-dimensional form are

$$u(y = h_1) = -1 = u(y = h_2) \tag{12a}$$

$$-\tau(y = \lambda_1) = \tau_y = \tau(y = \lambda_2) \tag{12b}$$

$$u(y = \lambda_1) = u_p = u(y = \lambda_2) \tag{12c}$$

The instantaneous wall flux Q(X , t) across the channel in fixed frame is given by

$$Q = \int_{h_2}^{h_1} U\, dY \tag{13}$$

If q is the rate of flow independent of x and t in wave frame then

$$q = \int_{h_2}^{h_1} u\, dy \tag{14}$$

It follows that $Q = q + h_1 - h_2$

The average volume flow rate over one period ($T = \frac{\lambda}{c}$) of the peristaltic wave is defined as

$$\bar{Q} = \frac{1}{T}\int_0^T Q\, dt = \frac{1}{T}\int_0^T [q + h_1 - h_2]\, dt = q + 1 + d \tag{15}$$

Method of solution

The solution of (10) using (12b) is given by

$$\tau = -\frac{dp}{dx}(y - \Lambda) \tag{16}$$

where $\Lambda = \left(\frac{\lambda_1 + \lambda_2}{2}\right)$ (17)

Using (16) and (12b), we obtain

$$\frac{\lambda_2 - \lambda_1}{2} = \beta \tag{18}$$

where

$$\beta = \tau_y / (-\frac{dp}{dx}) \tag{19}$$

is the half width of the plug flow region.

Substituting the expression for τ from (16) in the constitutive equation (11) and integrating with the help of boundary conditions (12a) we obtain the velocity distribution in different regions as

$$u(y) = u^-(y) = -1 - \frac{dp}{dx}\left\{(\Lambda+\beta)(y-h_2) - \right.$$
$$-\frac{1}{2}\left(y^2 - h_2^2\right) + \frac{4}{3}\sqrt{\beta}\left[(\Lambda - y)^{3/2} - \right. \tag{20a}$$
$$\left.\left. -(\Lambda - h_2)^{3/2}\right]\right\} \quad for\ h_2 \le y \le \lambda_1$$

$$u(y) = u_p = \text{constant} \qquad \text{for } \lambda_1 \le y \le \lambda_2 \tag{20b}$$

$$u(y) = u^+(y) = -1 - \frac{dp}{dx}\left\{\frac{1}{2}\left(h_1^2 - y^2\right) + \right.$$
$$+(\beta - \Lambda)(h_1 - y) - \frac{4}{3}\sqrt{\beta}\left[(h_1 - \Lambda)^{3/2} - \right. \tag{20c}$$
$$\left.\left. -(y - \Lambda)^{3/2}\right]\right\} \qquad for \quad \lambda_2 \le y \le h_1$$

where u^-, u^+ represent the velocity in shear flow regions $h_2 \le y \le \lambda_1$ and $\lambda_2 \le y \le h_1$ respectively and u_p represents the velocity in the plug flow region $\lambda_1 \le y \le \lambda_2$ which can be determined from (12c). As $\beta \to 0$, corresponding to the Newtonian fluid and a = b, d = 1, ϕ =0 in a symmetric channel case, the expression for axial velocity agrees with the expression obtained by Shapiro *et al.*[17].

The continuity condition (12c) for velocity distribution at the interfaces $y = \lambda_1$ and $y = \lambda_2$ gives the relation

$$\left[(\lambda_1 + \lambda_2) - (h_1 + h_2)\right] \times$$
$$\times\left[\frac{h_1 - h_2}{2} + \beta\right] + \frac{4}{3}\sqrt{\beta}\left[(\Lambda - \lambda_1)^{3/2} - \right. \tag{21}$$
$$\left. -(\Lambda - h_2)^{3/2} + (h_1 - \Lambda)^{3/2} - (\lambda_2 - \Lambda)^{3/2}\right] = 0$$

The relations (18) and (21) constitute a system of equations in two unknowns λ_1 and λ_2. We can determine λ_1 and λ_2 from these two equations with the help of the relation $\Lambda = \left(\frac{\lambda_1 + \lambda_2}{2}\right)$.

The transverse velocity v and the stream-function ψ are calculated (Appendix A). The expression for ψ in symmetric channel case agrees with that obtained by Mernone *et al*[12]. As $\beta \to 0$, (Newtonian case) we have $\lambda_1 = \lambda_2 = \frac{h_1 + h_2}{2}$ and in this case the stream-function agrees with the expression given by Mishra and Rao[13], when β = 0, and a = b, d = 1, ϕ = 0 (corresponding to the Newtonian fluid flow in a symmetric channel case) the stream-function matches with that of Shapiro *et al.*[16]. The pressure rise per wavelength and the dimensionless time mean flow are calculated (Appendix B).

Results and discussion

The peristaltic transport of a Casson fluid in a two-dimensional asymmetric channel in a wave frame is investigated under the long wavelength and low-Reynolds number assumptions. The analysis is relevant in the study of peristaltic transport of some physiological fluids such as urine in the ureter under certain pathological conditions and blood in small vessels. The results of the flow characteristics for different values of the parameters are discussed below.

Yield plane locations

The effect of yield stress is that the fluid exhibits a solid-like behaviour (or a plug core) in a region where the magnitude of the shear stress is less than the value of yield stress. The location of a point where the magnitude of actual shear stress is equal to the yield value, called a yield point and the locus of all such points is the yield plane. In view of the asymmetry in the two boundary walls the location of the two yield planes are calculated. These two yield planes determine the width of the core region. From equation (19) it is seen that the width 2β of the plug flow region depends on the shear stress τ_y and the pressure gradient and is independent of the asymmetry of the walls. The locations of the yield planes versus x are plotted in fig. 2. It is seen from fig. 2a, that the yield plane locations in a symmetric channel (for a = 0.5, b = 0.5, d = 1, ϕ = 0) are symmetrically located on either side of the centreline y = 0. When the asymmetry in the boundary (Fig. 2b) is considered taking two different amplitudes of the waves (a = 0.5, b = 0.7, ϕ = 0) the yield plane locations are no more symmetric and the plug region is skewed towards the boundary wall with higher amplitude. When there is a phase difference in the waves (fig. 2c) the plug region is found to be skewed towards the boundary having a phase difference.

Table 1 shows the location of the first yield plane λ_1 with phase angle ϕ of the wave imposed on the lower wall. The location of the second yield plane λ_2 can be calculated from table 1 and using the relation given by (18). It is observed from the table that as ϕ increases for a fixed value of τ_y the location of yield plane (λ_1) shifts towards the upper boundary and as τ_y increases, the width of the plug region increases.

Velocity distribution

Fig.3a shows the axial velocity distribution in a symmetric channel (a = b = 0.5, d = 1.0, ϕ = 0) and fig.3b shows the distribution in an asymmetric channel. The velocity in a symmetric channel is seen to be symmetric while the profiles are skewed towards lower boundary in an asymmetric channel. As the yield stress increases we notice that there is a reduction in the magnitude of the velocity and the plug flow dominates over the cross section.

Pressure rise and flux

The condition $\Delta P = 0$ is called as free pumping, when

ϕ \ τ_y	0.0	0.05	0.1	0.15	2.0	2.5
0	0.000	-0.05	-0.100	-0.150	-2.00	-0.250
$\pi/6$	0.033	-0.016	-0.066	-0.116	-0.166	-0.216
$\pi/3$	0.125	0.075	0.025	-0.025	-0.075	-0.125
$\pi/2$	0.250	0.200	0.150	0.100	0.050	0.000
$2\pi/3$	0.376	0.325	0.275	0.225	0.175	0.125
$5\pi/6$	0.466	0.416	0.366	0.316	0.266	0.216
π	0.500	0.450	0.4	0.350	0.300	0.250

Table 1. *Variation of yield plane location λ_1 with phase difference of the wave when the amplitudes of the waves are same (a = 0.5, b = 0.5, d = 1) for different values of yield stress.*

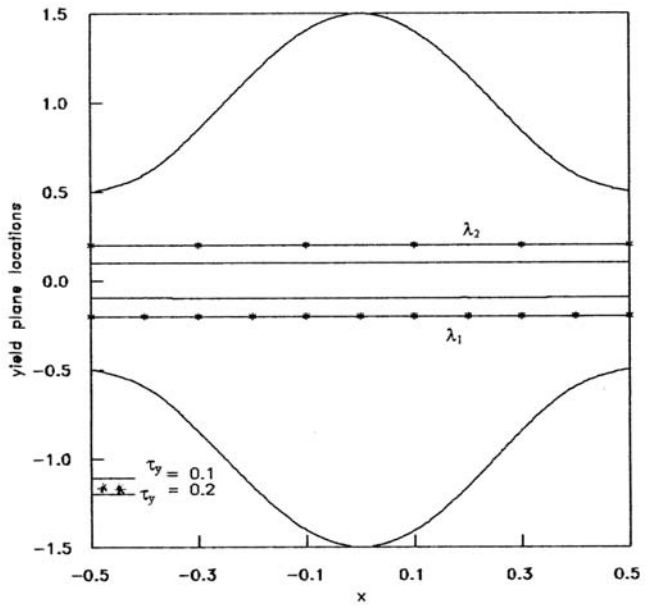

(a)

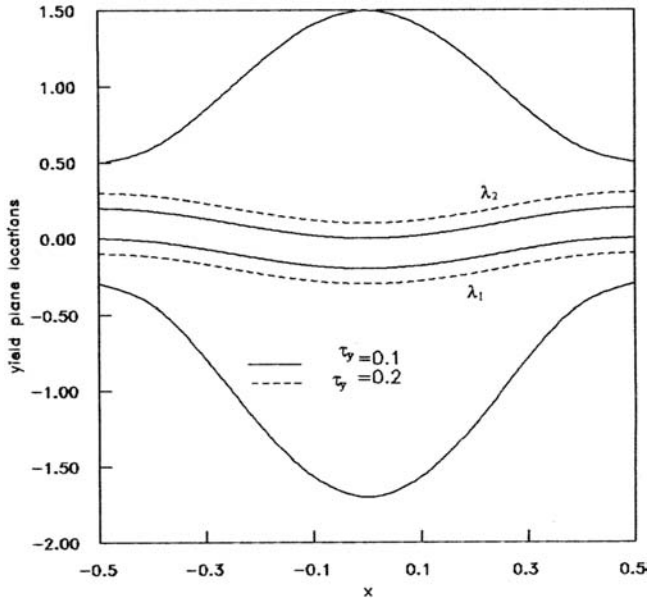

(b)

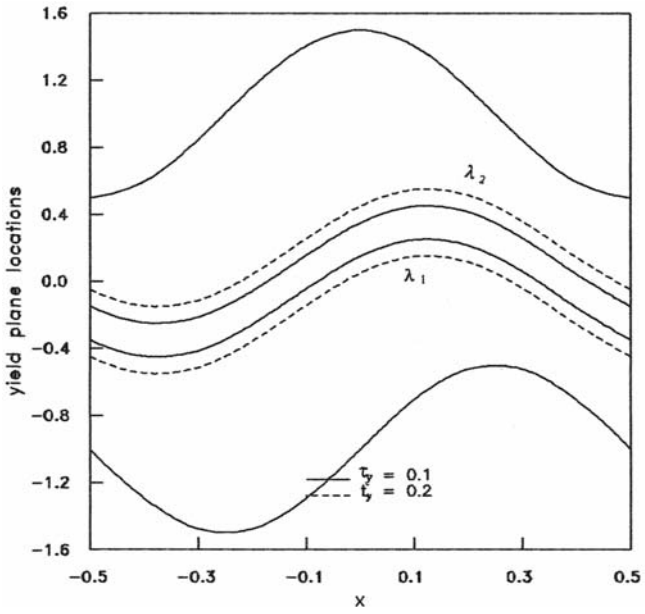

(c)

Figure 2. (a) *Variation of yield plane locations with x when a = b = 0.5, d = 1, ϕ = 0.0, (b) Variation of yield plane locations with x when a = 0.5, b = 0.7, d = 1, ϕ = 0.0, (c) Variation of yield plane locations with x when a = b= 0.5, d = 1, ϕ = 1.57.*

$\Delta P > \Delta P_0$ negative flux occurs, when $\Delta P < 0$ pressure also assists the flow and we have $\overline{Q} > \overline{Q}_0$. In this case it is known as copumping. The variation of time-average flux as a function of the normalized phase difference ($\overline{\phi} = \frac{\phi}{\pi}$) is calculated from equation (B3). The plot of the time average flux versus $\overline{\phi} = \frac{\phi}{\pi}$ is shown in figs. 4a and 4b. When the amplitudes of the peristaltic waves of the upper and lower walls are the same it is observed that the time average flux is maximum at $\overline{\phi}$ = 0 and decreases with $\overline{\phi}$ for all values of ΔP. When yield stress is present, during copumping it is seen that $\overline{Q}$ is positive for all values of $\overline{\phi}$ as in the case of Newtonian fluid. In the case of free pumping $\overline{Q}$ decreases

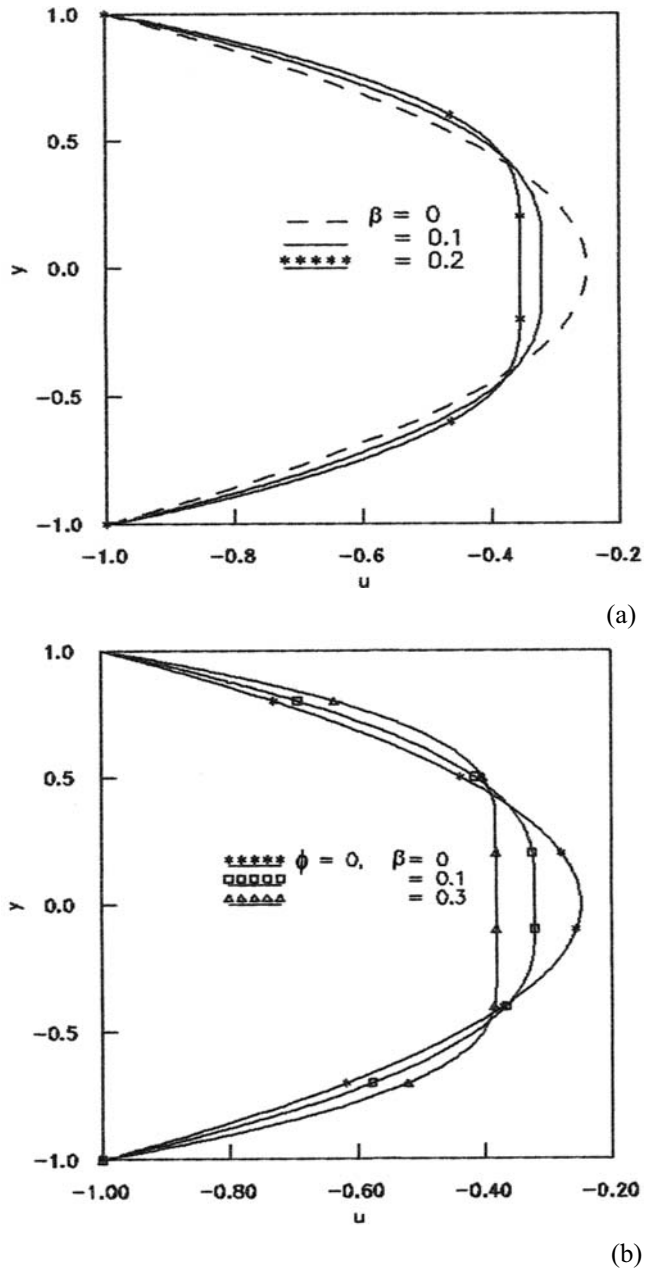

Figure 3. *(a) Variation of axial velocity with y when a = b = 0.5, d = 1, ϕ = 0.0, $\overline{Q}$ = 1.0, x = 0.25, (b) Variation of axial velocity with y when a = 0.5, b = 1.2, d = 1, $\overline{Q}$ = 1.0, x = 0.25*

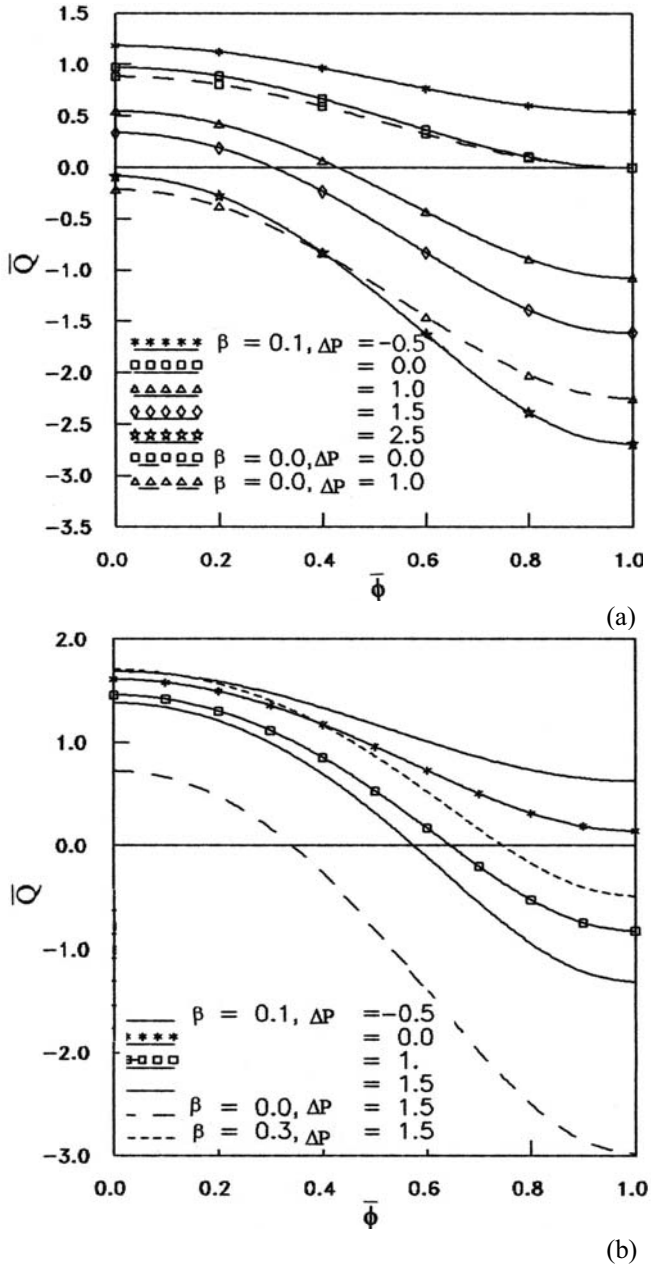

Figure 4. *(a) Variation of $\overline{Q}$ with $\overline{\phi}$ for different ΔP when a = b= 0.7, d = 2.0, (b) Variation of $\overline{Q}$ with $\overline{\phi}$ for different plug width and ΔP when a = 0.7, b = 1.2, d = 2.0.*

from its maximum value (0.7409) at $\overline{\phi} = 0$ as $\overline{\phi}$ increases and approaches zero value at $\overline{\phi}$ = 1. When $\Delta P = 1$, $\overline{Q}$ decreases from its maximum at $\overline{\phi} = 0$ and becomes zero at $\overline{\phi} = 0.42$ and it remains negative for the remaining values of $\overline{\phi}$ until it assumes the value 1. For ΔP = 1.5 the behaviour of $\overline{Q}$ is similar to the case when ΔP = 1.0. The positive flux for $0 \le \Delta P \le \Delta P_0$ is purely due to peristalsis. When ΔP = 2.5 the average flux is totally negative. In the case of Newtonian fluid $\overline{Q}$ becomes totally negative when ΔP = 1.0 . The effect of yield stress on $\overline{Q}$ is significant when ΔP > 0 while it has less effect during pumping and copumping (i.e. $\Delta P \le 0$) . The effect of yield stress on $\overline{Q}$ is significant at $\overline{\phi} = 0$. In the case of free pumping at $\overline{\phi} = 0$, $\overline{Q}$ decreases from 0.9716 (β = 0.1) to 0.8839 in the case of Newtonian fluid when β = 0 and then approaches zero as $\overline{\phi} \to 1$. When the amplitudes of the two peristaltic waves are different (fig. 4b), the time average flux is totally positive during copumping and pumping for all values of $\overline{\phi}$. When ΔP = 1.5 the flux is seen to be

positive when $0 \leq \bar{\phi} \leq 0.37$ in the case of a Newtonian fluid ($\beta = 0$). It is interesting to note that the presence of yield stress increases the magnitude of $\bar{Q}$ and is positive for a wider range of the values of $\bar{\phi}$. As the yield stress increases $\bar{Q}$ is observed to be increasing. From fig. 5a it is seen that $\bar{Q}$ increases with ϕ during copumping. When $\phi = \pi$, a = 0.7, b = 1.2, d = 2 (fig. 5b) it is found that in copumping the presence of yield stress and increase in yield stress decreases $\bar{Q}$. When $\Delta P > 0$, contrast behaviour is noticed. During pumping $\bar{Q}$ assumes almost same values in the presence and in the absence of yield stress.

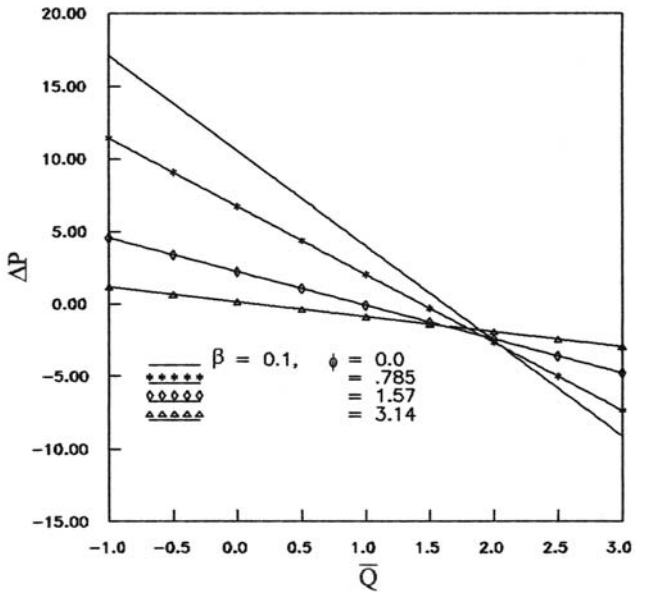

(a)

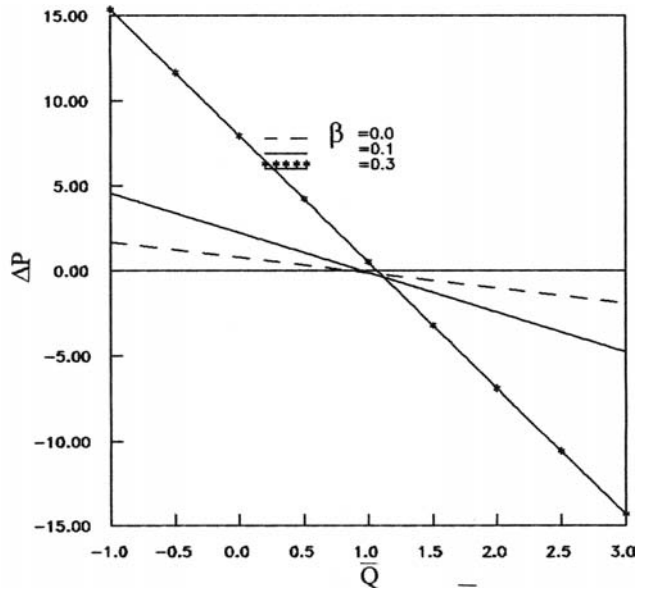

(b)

Figure 5. *(a) Variation of ΔP with flux $\bar{Q}$ for different ϕ when a = 0.7, b = 1.2, d = 2, β = 0.1, (b) Variation of ΔP with flux $\bar{Q}$ for different β when a = 0.7, b = 1.2, d = 2, ϕ = 1.57.*

Streamlines and trapping

The streamline pattern for a variation in the volume flow rate is shown in fig. 6. It is seen from fig. 6 (a = b = 0.5, d =1.0, $\phi = 0$, $\beta = 0.1$), when $\bar{Q} = 1.7$ the trapping of fluid bolus sets in near the centreline. For $\bar{Q} = 1.8$ the volume of the trapped bolus increases. When $\bar{Q} = 2.0$ we notice total recirculation zones. For further increases in $\bar{Q}$ the volume of the recirculation zones reduce, a shift towards the boundary is noticed and trapping disappears when $\bar{Q} = 2.8$ (fig. 7). For small amplitudes (a= b = 0.1) we observe that there is no fluid trapping (fig. 8a). When the amplitude of the peristaltic wave is 0.3 (fig. 8b)

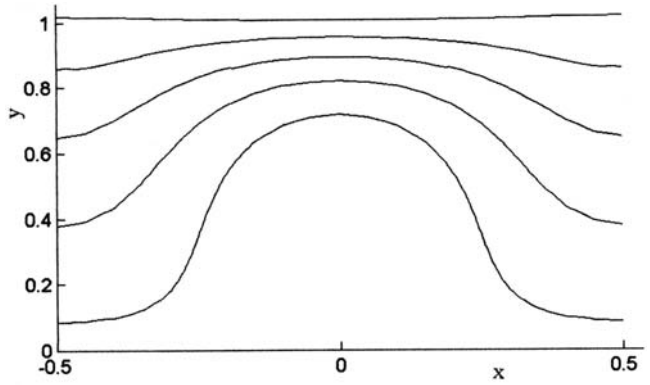

(a)

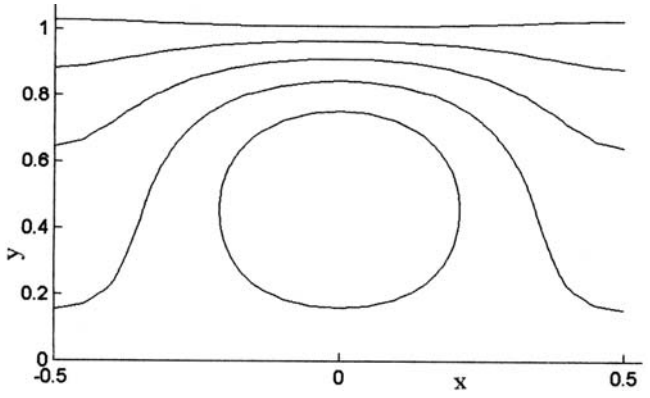

(b)

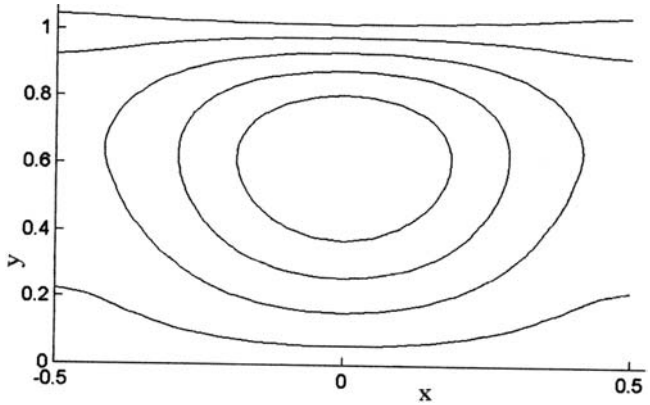

(c)

Figure 6. *Streamlines for a = b = 0.5, d = 1, $\phi = 0$, $\beta = 0.1$. (a) $\bar{Q} = 1.7$, (b) $\bar{Q} = 1.8$, (c) $\bar{Q} = 2$.*

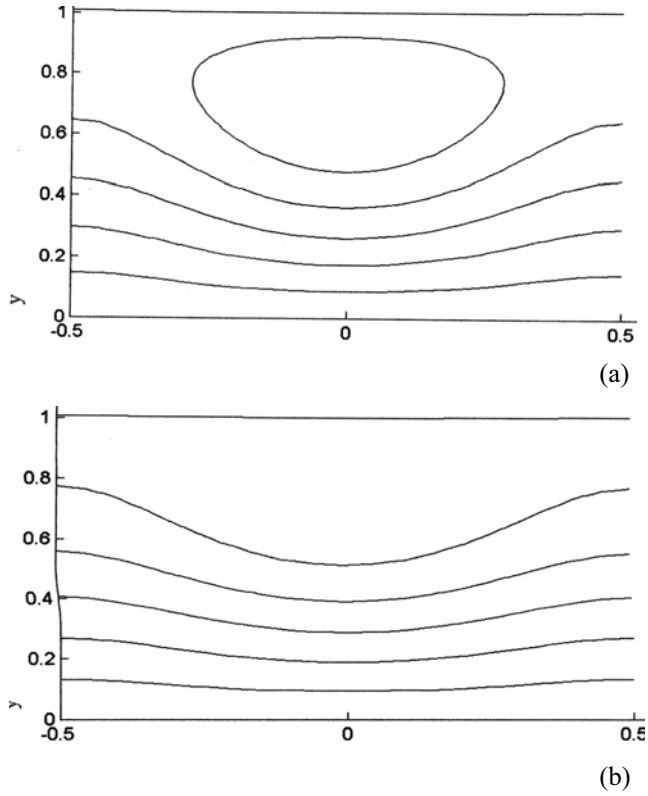

Figure 7. *Streamlines for a = b = 0.5, d = 1, ϕ = 0, β = 0.1. (a) $\overline{Q}$ = 2.4, (b) $\overline{Q}$ = 2.8.*

trapping occurs and the volume of the trapped bolus increases with the amplitude (fig.8c, when a = b = 0.5, d = 1.0, $\overline{Q}$ = 2.2, β = 0.1, ϕ = 0).

Reflux phenomenon

The phenomenon reflux means that the existence of mean motion of some fluid particles over a cycle against the net pumping direction. Since the flow in fixed frame is unsteady the path lines of the material particle are different from streamlines while in the moving frame path lines and streamlines coincide as the flow becomes steady. They are similar to the wall shape, but with lesser amplitude near the axis. Following Shapiro *et al.*[16], Q_ψ defined as dimensionless volume flow rate in the fixed frame between the centreline of the channel $\frac{h_1 + h_2}{2}$ and the wave streamline ψ, which is an indicator of material particles in fixed frame, is given by

$$Q_\psi = \int_{\frac{h_1+h_2}{2}}^{Y(\psi, X, t)} U(X,Y,t)\ dY \qquad (22)$$

By using the transformation between fixed frame and wave frame given in equation (7) and integrating (30), we get

$$Q_\psi = \psi + y(\psi, X, t) - \frac{h_1 + h_2}{2} \qquad (23)$$

Averaging over the one period of the wave

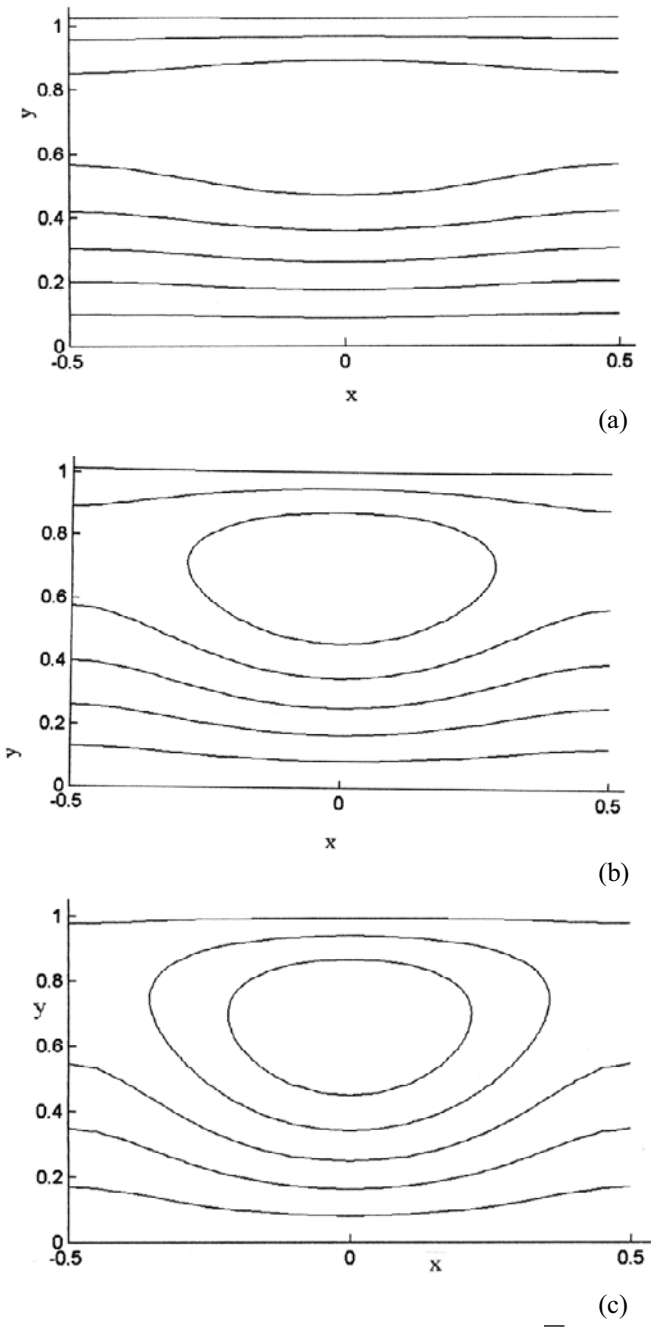

Figure 8. *Streamlines for d = 1, ϕ = 0, β = 0.1, $\overline{Q}$ = 2.2. (a) a = b = 0.1, (b) a = b = 0.3 (c) a = b = 0.5.*

$$\overline{Q}_\psi = \psi + \int_0^1 y(\psi, x)\ dx - \frac{1-d}{2} \qquad (24)$$

Defining $Q^* = \overline{Q}_\psi / \overline{Q}_w$, $\psi^* = \psi / \psi_w$, where $\overline{Q}_w$ and ψ_w are the values of $\overline{Q}_\psi$ and ψ at the wall y = h_1, $\overline{Q}_w = \overline{Q}/2$ and $\psi_w = (\overline{Q} - 1 - d)/2$. According to Shapiro *et al.*[16] reflux layer exists near the wall, whenever Q^* increases to a value greater than one and decreases to one at the wall. Following the analysis of Shapiro *et al.*[16] expressing y in terms of ψ using (A3c) and giving expansion in small amplitudes the integrand of (24) is

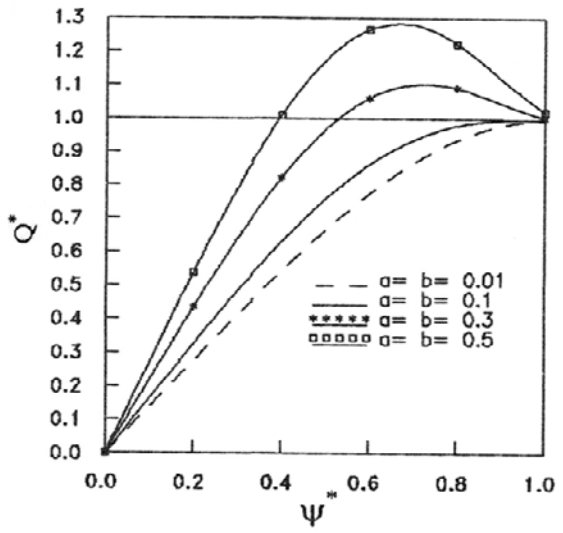

(a)

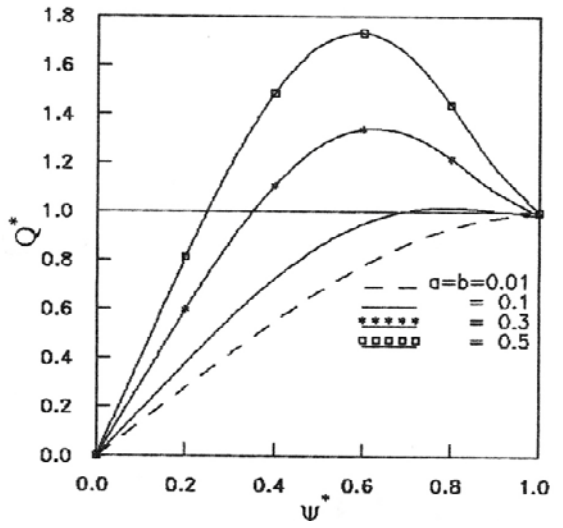

(b)

Figure 9. *(a) Variation of Q^* with ψ^* when $\beta = 0.1$, $\overline{Q} = 0.1$, $d = 1$, $\phi = 0$, (b) Variation of Q^* with ψ^* when $\beta = 0.1$, $\overline{Q} = 0.05$, $d = 1$, $\phi = 0$*

calculated. The integral is evaluated numerically by using Simpson's rule.

Fig. 9a depicts the variation of Q^* as a function of ψ^* for different amplitudes of the peristaltic wave for a = b, d = 1, $\phi = 0$, $\beta = 0.1$, $\overline{Q} = 0.1$. It is observed that there is no reflux for small values of the amplitude. Reflux is seen to occur for higher values of amplitudes ($a \geq 0.3$) and the reflux zone extends with an increase in amplitude. In fig. 9b the variation of Q^* for a variation in amplitudes, when $\overline{Q}$ is half of the value considered in fig. 9a. It is found that reflux occurs even for small amplitude i.e. a = 0.1. In this case for higher values of the amplitude, the reflux zones are doubled to those in the case of fig. 9a.

The reflux limits are obtained (Appendix C). In a symmetric channel (a = b, d = 1, $\phi = 0$), for a Newtonian fluid ($\beta = 0$), the reflux limits are found to agree with those obtained by Mishra and Rao[13].

Conclusions

The peristaltic transport of a Casson fluid in an asymmetric channel is studied in the wave frame under long wavelength and low Reynolds number assumption. Due to the asymmetry in the channel, the yield stress of the fluid tends to form two yield planes in the plug core region. When the channel is symmetric the yield planes are found to be located symmetrically on either side of the centreline y = 0 and in an asymmetric channel the plug region is skewed towards the boundary wall with higher amplitude (or phase difference). The presence of yield stress is found to enhance the time average flux. It is noticed that trapping of fluid flows occurs and the trapping zone extends for an increase in the time average flux ($\overline{Q} = 2.0$) and it disappears for $\overline{Q} = 2.8$. In the case of channel symmetry, reflux occurs for higher values of amplitude of the peristaltic wave and the reflux zone extends for an increased in the amplitude. The model can further be redefined by considering the effects of the elasticity of the walls, which will effect the yield plane locations and flow characteristics.

Acknowledgements

The authors are thankful to the referees for their constructive suggestions.

Appendix A

We may calculate the transverse velocity v from the equation of continuity

$$\frac{\partial v}{\partial y} = -\frac{\partial u}{\partial x} \qquad \text{(A1)}$$

Defining the stream function as

$$d\psi = u\,dy - v\,dx \qquad \text{(A2)}$$

and using the conditions $\psi = \frac{q}{2}$ at $y = h_1$ $\psi = -\frac{q}{2}$ at $y = h_2$ we obtain the stream-function in the three regions as

$$\psi_1 = -y - \frac{dp}{dx}\left\{(\Lambda+\beta)\left(\frac{y^2}{2}-h_2\, y\right) - \frac{1}{2}\left(\frac{y^3}{3}-h_2^2\, y\right) - \frac{4}{3}\sqrt{\beta}\left[\frac{2}{5}(\Lambda - y)^{5/2} + (\Lambda - h_2)^{\frac{3}{2}} y\right]\right\} + C_1$$

for $h_2 \le y \le \lambda_1$ (A3a)

$$\psi_p = u_p\, y + C_p \quad \text{for} \quad \lambda_1 \le y \le \lambda_2 \tag{A3b}$$

$$\psi_2 = -y - \frac{dp}{dx}\left\{\frac{1}{2}\left(h_1^2\, y - \frac{y^3}{3}\right) + (\beta - \Lambda)\left(h_1 y - \frac{y^2}{2}\right) - \frac{4}{3}\sqrt{\beta}\left[(h_1-\lambda)^{\frac{3}{2}} y - \frac{2}{5}(y-\Lambda)^{\frac{5}{2}}\right]\right\} + C_2$$

for $\lambda_2 \le y \le h_1$ (A3c)

where

$$C_1 = \frac{-q}{2} + h_2 + \frac{dp}{dx}\left\{\frac{-\Lambda h_2^2}{2} + \frac{h_2^3}{3} - \frac{\beta h_2^2}{2} - \frac{4}{15}\sqrt{\beta}(\Lambda - h_2)^{\frac{3}{2}}(2\Lambda + 3h_2)\right\}$$

$$C_p = -\frac{q}{2} + h_2 - \frac{dp}{dx}\left\{(\Lambda+\beta)\left(\frac{h_2^2 - \lambda_1^2}{2}\right) + \frac{1}{3}\left(\lambda_1^3 - h_2^3\right) - \frac{4}{15}\sqrt{\beta}\left[(\Lambda-\lambda_1)^{\frac{3}{2}}(2\Lambda+3\lambda_1) - (\Lambda - h_2)^{\frac{3}{2}}(2\Lambda+3h_2)\right]\right\}$$

$$C_2 = \frac{q}{2} + h_1 + \frac{dp}{dx}\left\{\frac{h_1^3}{3} + (\beta-\Lambda)\frac{h_1^2}{2} - \frac{4}{15}\sqrt{\beta}\,(h_1-\Lambda)^{\frac{3}{2}}(3h_1+2\Lambda)\right\}$$

Appendix B

The pressure gradient is obtained by using (14) as

$$\frac{dp}{dx} = -\frac{(q + h_1 - h_2)}{F(x)} \tag{B1}$$

where

$$F(x) = \frac{1}{3}\left(h_1^3 - h_2^3 + \lambda_1^3 - \lambda_2^3\right) + \frac{\Lambda}{2}\left(h_2^2 - h_1^2 + \lambda_2^2 - \lambda_1^2\right) + \frac{\beta}{2}\left(h_1^2 + h_2^2 - \lambda_1^2 - \lambda_2^2\right) - \frac{4}{15}\sqrt{\beta}\left[(\Lambda - \lambda_1)^{\frac{3}{2}}(2\Lambda + 3\lambda_1) - (\Lambda - h_2)^{\frac{3}{2}}(2\Lambda + 3h_2) + (h_1 - \Lambda)^{\frac{3}{2}}(3h_1 + 2\Lambda) - (\lambda_2 - \Lambda)^{\frac{3}{2}}(2\Lambda + 3\lambda_2)\right]$$

The pressure rise per wavelength is given by

$$\Delta P = \int_0^1 \frac{dp}{dx}\, dx = (1 + d - \overline{Q})\, I_1 + I_2 \tag{B2}$$

where

$$I_1 = \int_0^1 \frac{1}{F(x)}\, dx \quad , \qquad I_2 = \int_0^1 \frac{h_2 - h_1}{F(x)}\, dx$$

and $\overline{Q}$ can be written as

$$\overline{Q} = (1 + d) + \frac{I_2}{I_1} - \frac{\Delta P}{I_1} \tag{B3}$$

The dimensionless time mean flow $\overline{Q}_0$ for zero pressure rise is given by

$$\overline{Q}_0 = (1 + d) + \frac{I_2}{I_1} \tag{B4}$$

Also the dimensionless pressure rise for zero time mean flow is obtained as

$$(\Delta P)_{\overline{Q}=0} = \Delta P_0 = (1 + d)\, I_1 + I_2 \tag{B5}$$

Appendix C

The reflux limits may be obtained as follows. We consider wave frame streamlines close to the wall and introduce a small parameter

$$\delta = \psi - \psi_w = \psi - \frac{(\overline{Q} - 1 - d)}{2} \tag{C1}$$

The equation of streamline near the wall may be expressed as

$$y = h_1(1 + \delta a_1 + \delta^2 a_2 + ...) \tag{C2}$$

Substituting (C1) and (C2) in (A3c) we obtain

$$a_1 = -\frac{1}{h_1} \tag{C3}$$

$$a_2 = \frac{1}{2h_1}\frac{dp}{dx}\left[h_1 - \Lambda + \beta - 2\sqrt{\beta}\,(h_1 - \Lambda)^{1/2}\right] \tag{C4}$$

and hence y can be written as

$$y = h_1 - \delta + \frac{\delta^2}{2}\frac{dp}{dx}\left[h_1 - \Lambda + \beta - 2\sqrt{\beta}\,(h_1 - \Lambda)^{1/2}\right] + \tag{C5}$$

Substituting (C5) in (24) we obtain

$$\overline{Q}_\psi = \frac{\overline{Q}}{2} - \frac{1}{2}\delta^2 \int_0^1 \left[\frac{(Q - 1 - d + h_1 - h_2)}{F(x)} - [h_1 - \lambda + \beta - 2\sqrt{\beta}\,(h_1 - \Lambda)^{\frac{1}{2}}]\right] dx \tag{C6}$$

Using this, we obtain

$$\frac{\overline{Q}_{\psi}}{\overline{Q}_{w}} = 1 - \frac{\delta^2}{\overline{Q}} \int_0^1 \left[\frac{\left(\overline{Q} - 1 - d + h_1 - h_2\right)}{F(x)} \right.$$
$$\left. [\, h_1 - \lambda + \beta - 2\sqrt{\beta}\ \left(h_1 - \Lambda\right)^{\frac{1}{2}}\,] \right] dx \qquad \text{(C7)}$$

Reflux occurs when $\frac{\overline{Q}_{\psi}}{\overline{Q}_{w}} > 1$, from which the reflux limit is obtained as

$$\overline{Q} < \frac{\int_0^1 \frac{[1 + d + h_2 - h_1] G(x)}{F(x)}\, dx}{\int_0^1 G(x)/F(x)\, dx} \qquad \text{(C8)}$$

where

$$G(x) = \left[h_1 - \lambda + \beta - 2\sqrt{\beta}\ \left(h_1 - \Lambda\right)^{\frac{1}{2}} \right]$$

The same procedure can be repeated to obtain the limits near the other boundary wall $y = h_2$.

References

1. Aroesty, J. and Gross, J. F., *The mathematics of pulsatile flow in small blood vessels, I. Casson theory*. Microvasc. Res. 4: 1-12, 1972.
2. Aroesty, J. and Gross, J. F. *Pulsatile flow in small blood vessels I. Casson theory*, Biorheology 9: 33-42, 1972.
3. Bird, R. B., Stewart, W. E. and Lightfoot, E. N., *Transport Phenomena,* John Wiley and Sons, New York., 1960.
4. DeVries, K., Lyons, E. A., Ballard. J., Levi, C. S. and Lindsay, D. J., *Contractions of the inner third of the Myometrium*, Am. J. Obstetrics Gynecol. 162: 679-682, 1990.
5. Elshehawey. J. et al., *Peristaltic motion of generalized Newtonian fluid in a non-uniform channel,* J. Phys. Soc. Japan 67: 434- 440, 1998.
6. Eytan, O. and Elad, D., *Analysis of Intra-Uterine fluid motion induced by uterine contractions,* Bull. Math. Biology. 61: 221-238, 1999.
7. Fung, Y. C., *Biomechanics: Mechanical Properties of Living Tissue*, Springer Verlag, New York, 1981.
8. Fung, Y. C., *Biodynamics Circulation,* Springer Verlag, New York, 1984.
9. Latham, T. W., *Fluid motion in a peristaltic pump*, M. S thesis M. I. T., Cambridge, 1966.
10. Mernone, A. V. and Mazumdar J. N., *Mathematical Modelling of Peristaltic transport of a non-Newtonian Fluid*, Australasian J. Physical and Engineering Sciences in Medicine, 23, 3: 94-100, 1998.
11. Mernone, A. V. and Mazumdar, J. N., *Biomathematical modeling of physiological fluids using a Casson fluid with emphasis to peristalsis,* Australasian Physical and Engineering Sciences in Medicine, 23, 3:94-100, 2000.
12. Mernone, A. V. and Mazumdar, J. N., Lucas, S. K., *A Mathematical study of peristaltic transport of a Casson fluid,* Mathematical and Computer Modelling 35, 894 - 912, 2002.
13. Mishra, M. and Rao, A. R., *Peristaltic transport of a Newtonian fluid in an asymmetric channel,* ZAMP, 54, 532-550, 2003-5.
14. Pozrikidis, C., *A study of peristaltic flow*, J. Fluid Mech. 180: 515-527, 1987.
15. Raju, K. K. and Devanathan, R., *Peristaltic motion of a non-Newtonian fluid*. Rheol. Acta,11: 170-179, 1972.
16. Shapiro, A. H., Jaffrin, M. Y. and Weinberg, S. L., *Peristaltic Pumping with long Wavelengths at low Reynolds number*. J. Fluid Mech. 37: 799-825, 1969.
17. Srivastava, L. M., *Peristaltic transport of a Casson fluid*, Nig. J.Sci.Res.1: 71-82, 1987.
18. Srivastava, L. M. and Srivastava, V. P., *Peristaltic transport of blood: Casson model II,* J. Biomechanics 17: No.11: 821-829, 1984.
19. Siddiqui, A. M., Provost, A. & Schwarz W. H., *Peristaltic Pumping of a Second –Order Fluid in a Planar Channel*, Rheol Acta 30: 249-262, 1991.
20. Tang, D. and Rankin, S., *Numerical and asymptotic solutions for peristaltic motion of non-linear viscous flows with elastic boundaries. SIAM J. Sci. Compt.* 14: No.6: 300-1319, 1993.